International Journal of Navigation and Port Research
Vol.30, No.9 pp. 755~762, 2006 (ISSN-1598-5725)

Evaluation of the Behavior of Dredged Materials in Ocean Dumping Area

Seung-Chul Lee · Kang-Min Kim** · Hyung-Chul Kim*** · † Joong-Woo Lee*****

**Graduate school of Korea Maritime University, Busan 606-791, Korea*
***Seileng Engineering Co., Ltd. Shingil-dong Yeongdeungop-gu, Seoul 150-051, Korea*
****World construction Co., Ltd., Seoul 150-890, Korea*
*****Division of Civil and Environment System Engineering, National Korea Maritime University, Busan 606-791, Korea*

Abstract : *When we consider to develop a new harbor, the most important factor, we think, is the lowest water depth of waterway and approaching channel for safe navigation of vessel. The existing harbors have been being dredged to meet the international trend of jumbo sized vessels by adopting the new design criteria. As the dredged materials over the expected at the design level were common and there are still lack of land based reclamation area, we have no choice to discharge the dredged materials in open sea area. In this study, we analysed the behavior of discharged materials at the dumping area of offshore, which were collected from the dredging work at the waterway in Busan New Port. We measured the tidal currents and analyzed the waters of dumping site after the dumping work. These were used to evaluate the numerical models. Suspended Solids(SS) were introduced to the diffusion model. Because of the characteristic of the dumping site, the speed of initial diffusion and settle down of the discharged materials was so fast. Therefore, we believe that the dumped materials do not cause a significant impact to the marine environment.*

Key words : *Dredged material, Dumping area, Discharge, Field measurement, Tidal current, Diffusion, Settlement*

1. Introduction

The 5,000 TEU class containership belonged to the large ship no more than 10 years ago but the trend becomes more larger as the development of technology and rapid increase of oil price. In Busan New port, started with the arrival of 8,000TEU containership in August 2004, 10,000TEU class containership is expected to berth at Busan New port. This trend made change to the design depth of waterway and mooring basin of Busan New port from 15m to 18m. In order to treat the sulplus of dredged materials, offshore dumping area of the materials was declared. The dredged materials were discharged at the open sea under the condition of monthly based water quality monitoring.

As the small change of ocean environment might greatly affect to the marine ecology, the investigation on the behavior of discharged materials in open water could be one of the important analysis items. The analyzed diffusion pattern and behavior of discharged materials might be used in environmental impact study and as an evaluation index.

In this study, we had made field measurement on currents and water quality at the site of dumping area for the dredged materials from the waterway of Busan New port as shown in Fig. 1, together with the numerical analysis of currents and diffusion of discharged materials. The calculation area for tidal current simulation covers the eastern part of Geoje Island and southern part of west Busan for the coastal boundary and 30~40km away for open boundary, including 2km by 2km of the dumping area. The adopted area of study is 70km × 65km avoiding the impact of open boundary. The input source for diffusion of the dumped material was based on the monthly measured water samples and the expected SS from the dredged materials.

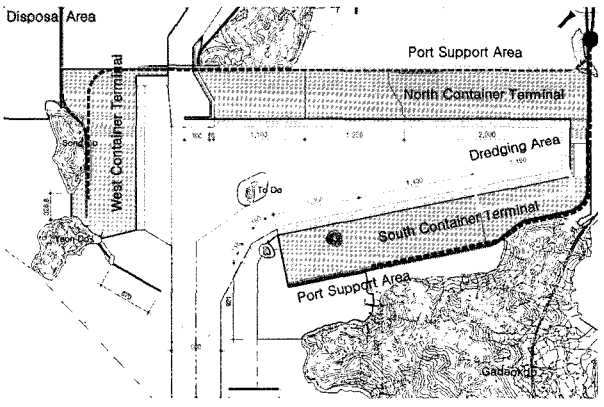

Fig. 1 Dredging area at the Busan New port

* Frist Author : Seung-Chol Lee, kmaritime99@nate.com 051)410-4981
** kikami@seileng.com 02)840-5182
*** kbwc2@worldro.co.kr 051)410-4981
† Corresponding Author : Joong-woo Lee, jwlee@mail.hhu.ac.kr 051)410-4461

The external forces for the diffusion simulation are tides and tidal currents from numerical simulation. We evaluated the diffusion simulation by comparision of the measured SS data after dumping work with the simulated ones.

2. Governing Equations

2.1 Currents and circulations

In this numerical study for the dynamics of coastal circulation the governing equations are the vertically integrated two-dimensional equations as follows. Simans (1974) and Madala & Piacsek(1977) had introduced a mode splitting technique at first, which the velocity transport was solved separately from the three-dimensional calculation of the velocity and the thermodynamic properties, permitting the calculations of the free surface elevation with no sacrifice in computation time. The vertically integrated equations were obtained by integrating the vertical structure equations over the depth.

The governing equations are converted to the sigma coordinates (x*, y*, σ, t*) from the conventional cartesian coordinates (x, y, z, t). Here, $x^* = x$, $y^* = y, \sigma = \frac{z-\eta}{H+\eta}$, $t^* = t$. Therefore, by integrating the equations of continuity and motion from $\sigma = -1$ to $\sigma = 0$ and applying the boundary conditions, the surface elevation and the momentum equations can be derived as

$$\frac{\partial \eta}{\partial t} + \frac{\partial \overline{U}D}{\partial x} + \frac{\partial \overline{V}D}{\partial y} = 0 \tag{1}$$

$$\begin{aligned}\frac{\partial \overline{U}D}{\partial t} &+ \frac{\partial \overline{U^2}D}{\partial x} + \frac{\partial \overline{U}\,\overline{V}D}{\partial y} - f\overline{V}D + gD\frac{\partial \eta}{\partial x} - D\overline{F_x} \\ &= -\overline{wu}(0) + \overline{wu}(-1) - \frac{\partial D\overline{U'^2}}{\partial x} - \frac{\partial D\overline{U'V'}}{\partial y} \\ &\quad - \frac{gD^2}{\rho_0}\frac{\partial}{\partial x}\int_{-1}^{0}\int_{\sigma}^{0}\rho d\sigma' d\sigma \\ &\quad + \frac{gD}{\rho_0}\frac{\partial D}{\partial x}\int_{-1}^{0}\int_{\sigma}^{0}\sigma'\frac{\partial \rho}{\partial \sigma}d\sigma d\sigma\end{aligned} \tag{2}$$

$$\begin{aligned}\frac{\partial \overline{V}D}{\partial t} &+ \frac{\partial \overline{U}\,\overline{V}D}{\partial x} + \frac{\partial \overline{V^2}D}{\partial y} + f\overline{U}D + gD\frac{\partial \eta}{\partial y} - D\overline{F_y} \\ &= -\overline{wv}(0) + \overline{wv}(-1) - \frac{\partial D\overline{U'V'}}{\partial x} - \frac{\partial D\overline{V'^2}}{\partial y} \\ &\quad - \frac{gD^2}{\rho_0}\frac{\partial}{\partial y}\int_{-1}^{0}\int_{\sigma}^{0}\rho d\sigma' d\sigma \\ &\quad + \frac{gD}{\rho_0}\frac{\partial D}{\partial y}\int_{-1}^{0}\int_{\sigma}^{0}\sigma'\frac{\partial \rho}{\partial \sigma}d\sigma d\sigma\end{aligned} \tag{3}$$

where, the vertically integrated velocities are defined as

$$(\overline{U}, \overline{V}) \equiv \int_{-1}^{0}(U, V)d\sigma \tag{4}$$

The wind stress components are $-\overline{wu}(0)$ and $-\overline{wv}(0)$, and the bottom stress components are $-\overline{wu}(-1)$ and $-\overline{wv}(1)$.

The terms $U'^2, U'V', V'^2$ of equations (2) and (3) are vertical mean of the fluctuation terms from the average velocities. Therefore, these represent the dispersion terms such as

$$(\overline{U'^2}, \overline{U'V'}, \overline{V'^2}) = \int_{-1}^{0}(U'^2, U'V', V'^2)d\sigma \tag{5}$$

where, $(U', V') = (U - \overline{U}, V - \overline{V})$.

The quantities $\overline{F_x}$ and $\overline{F_y}$ are the vertical integration of horizontal momentum diffusion terms and defined according to

$$D\overline{F_x} = \frac{\partial}{\partial x}(2A_M\frac{\partial \overline{U}D}{\partial x}) + \frac{\partial}{\partial y}A_M(\frac{\partial \overline{U}D}{\partial y} + \frac{\partial \overline{V}D}{\partial x}) \tag{6}$$

$$D\overline{F_y} = \frac{\partial}{\partial y}(2A_M\frac{\partial \overline{V}D}{\partial y}) + \frac{\partial}{\partial x}A_M(\frac{\partial \overline{U}D}{\partial y} + \frac{\partial \overline{V}D}{\partial x}) \tag{7}$$

The calculation schemes are complsed of the shallow wave equations (1) through (3) for tidal motion within short time steps which results in updates for surface elevations and the vertically averaged velocities. In this step the solutions for the right side of equations (2) and (3), and the solutions for the updates of surface elevation and velocity, and the turbulence quantities would be followed after 100 time steps.

When the numerical model is applied to the proposed site, the horizontal eddy viscosity coefficients might be used as constant but Smagorinsky type diffusive parameter (KORDI, 1993) which related with the grid size and velocity field is recognized better as following equation.

$$A_M = c\Delta x\Delta y\sqrt{\left(\frac{\partial U}{\partial x}\right)^2 + \frac{1}{2}\left(\frac{\partial U}{\partial y} + \frac{\partial V}{\partial x}\right)^2 + \left(\frac{\partial V}{\partial y}\right)^2} \tag{8}$$

here, c is a dimensionless constant, and △x, △y are grid size in x-direction and y-direction, respectively.

Therefore, we adopted the horizontal eddy viscosity coefficient as Smagorinsky type diffusive parameter considering the dispersion effect by vertical integration and used the same parameter for the horizontal turbulent diffusion coefficient.

The staggered grid was introduced using Arakawa C-grid for grid arrangement, and for the conservation of materials and energy the governing equations were converted to the finite difference equations in a flux-conservative form. The advective operators in these

equations are then written in a finite volume method for the conservation of materials and volumes. The surface elevation was calculated with the centered space accommodate the horizontal diffusion term whereas the leapfrog scheme is related to the time step. The centered space scheme was applied to the advective term of momentum equation and the backward space scheme was adopted to the continuity equation.

Although the leafrog scheme with three-time level is useful for time derivatives with Coriolis term, there appears a problem of time step splitting, where the physical mode is not coincide with the computation mode per each time step. Therefore, we applied Euler-backward scheme (Blumberg, 1977; Wang and Kravitz, 1980) and weak time filter (Blumberg and Mellor, 1987) to delete the instability due to the time-step splitting.

The time splitting in this study is removed at (n) time step by a weak filter (Asselin, 1972) where the solution is smoothed at each time step according to

$$T_s^n = T^n + \frac{\alpha}{2}(T^{n+1} - 2T^n + T_s^{n-1}) \tag{9}$$

where, T is the unsmoothed numerical solution and Ts is the smoothed solution, using α=0.05.

The Courant-Friedrichs-Lewy (CFL) computational stability condition on the vertically integrated governing equations limit the time step as (Blumberg and Mellor, 1987)

$$\Delta t \leq \frac{1}{C_t}\left(\frac{1}{\Delta x^2} + \frac{1}{\Delta y^2}\right)^{-1/2} \tag{10}$$

here, $C_t = 2\sqrt{gH} + U_{\max}$ and $U_{\max}$ is the expected mean maximum velocity.

In the model, we did not consider the effect of the wind stress and applied cold start for the coastal circulation simulation.

Lateral boundary conditions contiguous to coastlines were handled by setting to zero velocities normal to land boundaries. Quadratic stress law with Manning friction coefficient are applied to the bottom friction terms as

$$\vec{\tau} = C_D\sqrt{U^2 + V^2}\,\vec{U} \tag{11}$$

where, $C_D = gn^2\Delta z^{-1/3}$, n is the Manning's bottom friction coefficient, and Δz is the thickness of bottom layer (total water depth in case of depth averaged).

For open boundary condition of tide, combination of four tidal components (M2, S2, K1, O1) from the field measurements was introduced into the model as a function of time and space. On the otherhand, the open boundary condition of tidal current was introduced as follows: The momentum equations were solved for the velocities normal to the open boundary by neglecting the advective and the horizontal eddy viscosity terms, which needed the velocity components outside the open boundaries. For the tangential velocities at the open boundaries incoming from outside of the boundaries, they were assigned internal values adjacent to the open boundaries, but the following equation was used for the opposite direction.

$$\frac{\partial U_t}{\partial t} + U_n\frac{\partial U_t}{\partial x_n} = 0 \tag{12}$$

where, *Ut* is the tangential velocity component to the open boundary, *Un* and *xn* are the velocity component and the coordinate vertical to the open boundary, respectively.

2.2 Diffusion of the discharged materials

The used suspended solids transport model calculates the sedimentation and erosion rates, together with variation of SS diffusion, considering the suspension, advection, settling, and resuspension of dumped materials. The governing equation for SS transport is the two-dimensional continuity equation as

$$\frac{\partial C}{\partial t} + u\frac{\partial C}{\partial x} + v\frac{\partial C}{\partial y} = \frac{1}{h}\frac{\partial}{\partial x}\left(hD_x\frac{\partial C}{\partial x}\right) + \frac{1}{h}\frac{\partial}{\partial y}\left(hD_y\frac{\partial C}{\partial y}\right) + \sum_{i=1}^{n}\frac{S_i}{h} \tag{13}$$

where, C is the depth averaged concentration (g/m^3), u, v are the depth averaged velocities in x- and y-direction (m/s), D_x, D_y, dispersion coefficients (m^2/s), h, the water depth (m), and S_i, the sink and source terms at position i $(g/m^2/s)$.

Settling and resuspension of dumped materials are a function of the bottom shear stress (τ, N/m^2) such as

$$\tau = \rho g h\ J \tag{14}$$

where, ρ, the density of the sea water (kg/m^3), g, the gravitational force (m/s^2), J, the energy slope,

$$J = \frac{u^2 + v^2}{k^2 h^{4/3}} = \frac{u^2 + v^2}{Ch^2 h^2}$$

here, k, Strickler's roughness parameter $(m^{1/3}/s)$ and Ch, Chezy coefficient $(m^{1/2}/s)$.

The settlement of the suspended solids appears when the average velocity of flow is small enough compared with the

necessary allowed velocity for resuspension of the materials. The deposition rate D could be represented as

$$D=\frac{W_s C}{h_*}\left[\frac{\tau}{\tau_{cd}}-1\right], \tau \leqq \tau_{cd} \quad (15)$$

where, W_s, the settling velocity (m/s), h_*, the average settling depth (m), τ, the bottom shrear stress (N/m^2), and τ_{cd}, the critical bottom shear stress (N/m^2).

The resistance of the cohesive sediments to the erosion depends on not only for the immersed weight of each particle, but also the removal of the materials due to the electro chemical cohesion of each materials before the erosion start with the overcome of shear stress. Thus, the erosion rate E would be as shown as follows,

$$E=-\frac{M}{h}\left[\frac{\tau}{\tau_{ce}}-1\right], \tau \geqq \tau_{ce} \quad (16)$$

where, M, the constant for erosion and τ_{ce}, the limit bottom shear stress with respect to the erosion (N/m^2).

Erosion constant relies on the pattern of sediment transport, soil pressure, and salinity. As there is no general representation on M, it is frequently used as one of the compensation coefficients. The limit τ_{ce} was introduced as $0.5 N/m^2$.

The directional components for the diffusion coefficient k could be derived by transformation of the coordinates of streamline into the x-y cartesian coordinates. Those are represented with the direction of streamline, or current direction (ζ), and normal to this direction (η) as follows

$$k_{11}=\epsilon_\zeta \cos^2\theta+\epsilon_\eta \sin^2\theta \quad (17)$$

$$k_{12}=(\epsilon_\zeta-\epsilon_\eta)\cos\theta\sin\theta$$

$$k_{22}=\epsilon_\zeta \sin^2\theta+\epsilon_\eta \cos^2\theta$$

where, ϵ_ζ and ϵ_η are the mixing coefficients in the direction of current and normal to the current direction, respectively, Θ is angle between x and ζ axis (counter clock wise +), ϵ_ζ and ϵ_η are derived with the Elder's equation (Elder, 1959) in relation with the characteristics of the average currents as follows

$$\epsilon_\zeta=e_L U_* h, \quad \epsilon_\eta=e_T U_* h \quad (18)$$

where, e_L, e_T shows the dimensionless coefficients normal to each current direction (5.93 and 0.23, respectively by Elder's experiment)

3. Investigation of Field Environment

3.1 Waves

As per the report of short period wave measurement at Busan by MOMAF (1983), the occurrence rates of waves at the southern part of Jodo coastal sea showed 25.1% for over 0.5m of wave height, 8.3% for 0.5~0.9m, 6.1% for 1.0~1.9m, 0.7%(9 times annually) for 2.0~2.9m, and nothing for over 3.0m. The significant wave direction in this area was east appeared 15.9% and southeast was 9.2%. The analyzed wave periods were within 4.0~9.9sec. The dominant periods were in 6.0~7.9sec marked 9.9% and 8.0~9.9sec were 3.9% of total waves.

3.2 Tides

The tide shape factor for the vicinity of Gaduck Island is 0.15. It showed that the mixed tide but semi diurnal is dominant in this area. There are two highs and two lows in a day but the difference is not strong. The maximum appears at night during summer and daytime in winter. The lowest of the mean level appears in February to Mach and the highest in August to September.

The analyzed tidal range data in this area from the measurement in 1999 showed that the maximum 161.0cm, the mean 110.8cm, and the minimum 60.6cm, respectively. Comparing these with the maximum 166.0cm, the mean 113.4cm, and the minimum 60.8cm in 1978, we could see that there is no significant change.

The levels of App.HHOST, MHOST, and HHONT are 185.6cm, 173.3cm, and 123.1cm, respectively and about 2cm was lowered compared with the 1978's.

3.3 Tidal Currents

The analyzed maximum tidal currents at the site of dumping area showed about 50cm/sec from the field measurements during the period between December in 2005 and November in 2006 for the purpose of water quality investigation and there were minor differences between top and bottom. Fig. 2 indicates the averaged maximum tidal currents. The set up stations for current and water quality measurement including the suspended solids are shown in Table 1 and St. 5 is at the center and lest of points are 1 km away each other.

Table 1 Positions for the field measurement of tidal current and suspended solids

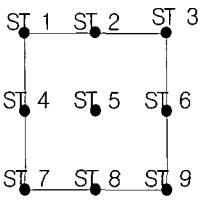

Station	N	E
ST. 1	34°50 ′ 32 ″	128°01 ′ 20 ″
ST. 2	34°50 ′ 32 ″	128°02 ′ 00 ″
ST. 3	34°50 ′ 32 ″	128°02 ′ 40 ″
ST. 4	34°50 ′ 00 ″	128°01 ′ 20 ″
ST. 5	34°50 ′ 00 ″	128°02 ′ 00 ″
ST. 6	34°50 ′ 00 ″	128°02 ′ 40 ″
ST. 7	34°49 ′ 28 ″	128°01 ′ 20 ″
ST. 8	34°49 ′ 28 ″	128°02 ′ 00 ″
ST. 9	34°49 ′ 28 ″	128°02 ′ 40 ″

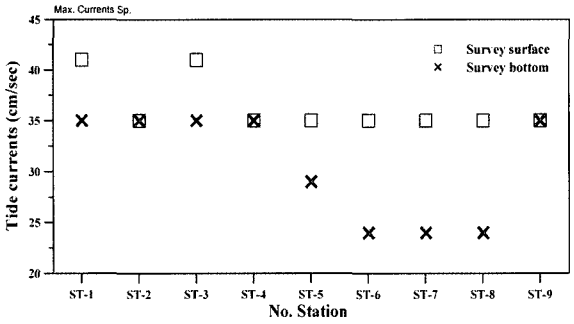

Fig. 2 Results of tide current survey (surface, bottom)

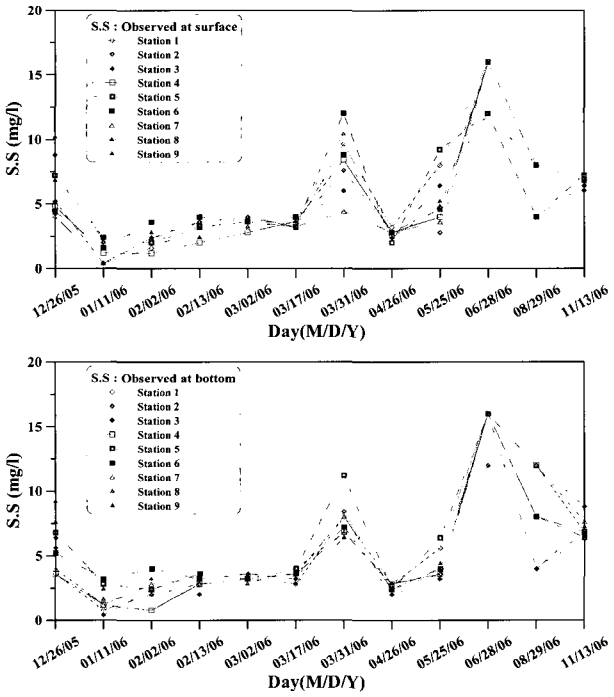

Fig. 3 Results of SS survey (Surface, Bottom)

3.4 Suspended Solids (SS)

As per the field measurements, the highest concentration of suspended solids was appeared in December in 2005, and March and June in 2006 as shown in Fig. 3. Except these the concentrations showed less than 10mg/L. There were no significant differences between top and bottom concentrations for each station due to the vertical circulation and diffusion. Furthermore, there were no significant difference on concentrations per different tidal phase, which were shown in the analysis of tidal currents.

4. Numerical Simulation

4.1 Summary of Experiment

In order to simulate the tidal circulation and diffusion of the dumped materials we set the coastal waters into the numerical model including the eastern part of Geoje Island and southern part of west Busan for the coastal boundary and 30~40km away for open boundary, neglecting the impact of the open boundaries. We adopted meshes of 50m interval near the dumping area (53km × 37.3km) to get high resolution and conducted simulations for 15 days which include the spring, neap, and medium tides. Table 2 shows the summary of model simulation set up. The variable mesh and water depth within the simulation area were shown in Fig. 4. PT-1 and PT-2 are observed tidal stations for verification of the model simulation.

For the input of diffusion simulation, we evaluated the SS source from the dumping rate of the dredged materials (13,916㎥/day) which were used in the environmental evaluation report of Busan New Port development plan. A summary of the input data were shown in Table 2.

Table 2 Summary of model simulation set up

Items		Simulation conditions
Tidal circulation	Cal. area	Eastern part of Geoje Island and southern part of west Busan (70.0km × 35.0km)
	Mesh scheme	338 × 267 (90,246개) △S=50,100,200,400,800,1600m Variable mesh
	Cal. time & friction	15days(M2+S2+K1+O1), n (friction coef.) : 0.023
SS diffusion	SS source	13,916㎥/day × 39.6kg/㎥ = 45,922.93kg/hr
	Concentration	Initial & Boundary value - 5mg/L
	Settling velocity	1.25mm/sec

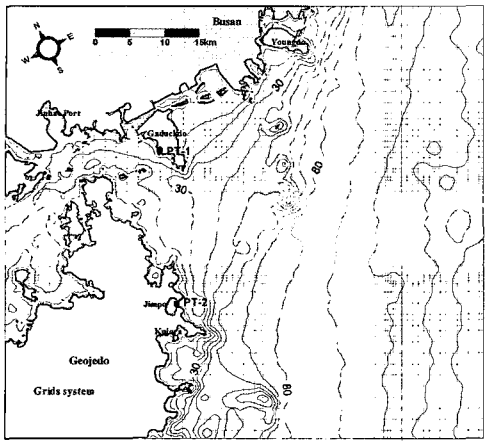

Fig. 4 Grids and bathymetric chart

4.2 Model Verification

In order to verify the numerical model we made comparison with the observed tides at PT-1 (Jisepo) and PT-2 (Gaduckdo). Furthermore, the maximum tidal currents were compared with the field measurements at the dumping sites. Fig. 5 shows the compared tidal elevations and the comparison of maximum tidal currents is shown in Fig. 6.

The compensated tidal elevations were matched to the measured with 96% of accuracy and the tidal currents were with over 72% of accuracy. The reason for the lower measured currents than the calculated is that each field measurement was done at the period between the spring and medium tides.

The calculated maximum flood and ebb currents are shown in Fig. 7. Ebb currents are slightly stronger than the flood currents in general.

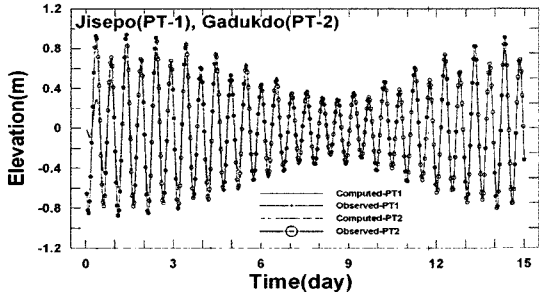

Fig. 5 Comparison of tidal elevations at PT-1 and PT-2

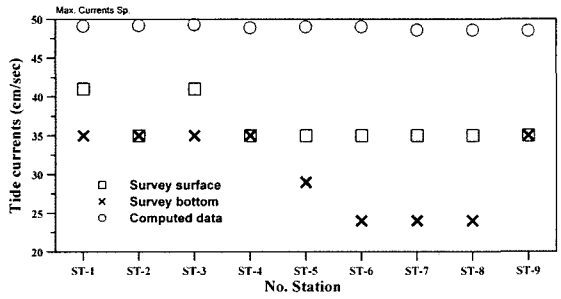

Fig. 6 Comparison of max. velocity on ST-1~9 point.

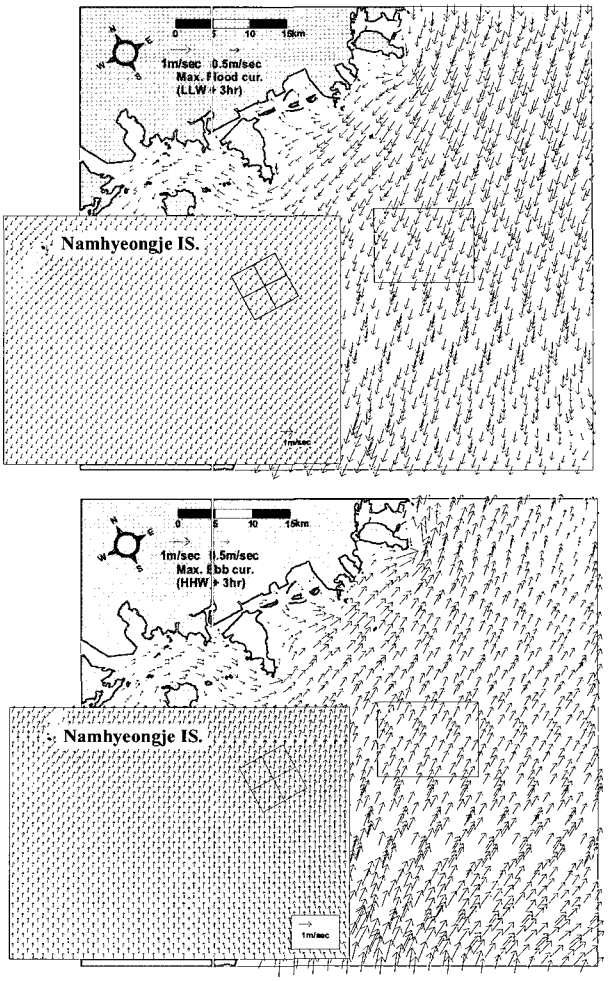

Fig. 7 Maximum flood and ebb currents

4.3 Simulation on Diffusion of SS

For the diffusion of suspended solids at the dumping site we conducted simulation for 15 days which covers the spring, medium, and neap tides. The maximum diffused boundaries by numerical calculations were based on the maximums at each grid for the given calculation times. The distribution of SS as shown in Fig. 8 is not at the same time period but indicate the possible maximum concentrations. The trend of diffusion shows that SS moves with the direction of flood and ebb currents, together with the slack time. The maximum boundary of 5mg/L concentration covers 284.02㎢. The maximum diffusion distance is 13.89km east direction and 11.89km south direction. We found the impact of flood current was slightly larger.

Fig. 9 shows the comparison of diffusion between SS survey and numerical model simulation 6 hours and 12 hours after the discharge of the dredged materials at the dumping site. The discrepancy comes from the difference of discharge pattern between two; a sudden dumping within 5 minutes in the field but continuous point sources in the numerical model. Therefore, it might be said that both the

distribution patterns of SS are agreed each other.

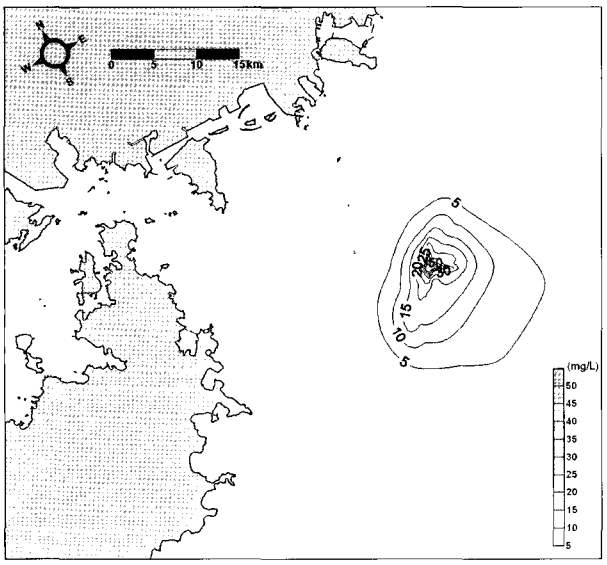

Fig. 8 Distribution of maximum SS concentration(mg/L)

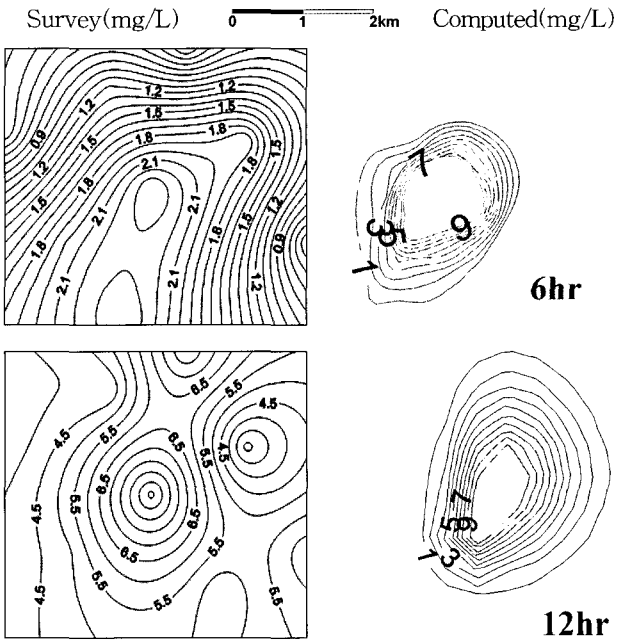

Fig. 9 Comparison of diffusion between survey and simulation

5. Conclusions

In this study we made numerical simulation on diffusion of SS due to the discharge of dredged materials at dumping site based on the result of 15 days tidal current simulations considering 4 main tidal components of M2, S2, K1, O1.

The verification of the formulated SS diffusion model relied on the stability of the original model. However, the result might be different depend on the user's approach to the formulation. It is thought be meaningful, therefore, that we tried to verify the numerical model with the use of the field measurement during the dumping period.

The summary of the result in this study is as follows:

1) The distribution of maximum currents during the spring tide at the dumping site showed less than 30-50cm/sec and ebb currents are slightly dominant compared with the flood currents.
2) From the spatial distribution of SS concentration by the analysis of the field measurement we found that diffusive mechanisms made almost even concentrations at the bottom and top of the water.
3) Although the diffusive patterns are similar between the field measurements and the numerical simulation results on temporal SS concentrations after discharge of the dredged materials, the exact amount of concentrations showed slightly different. This might come from the ratio of the SS source and the impact of water depth compared with the current in the open sea.
4) However it showed higher impacts on the maximum distribution of SS by the flood current.

References

[1] Blumberg, A. F. (1977), "Numerical model of estuarine circulation." Journal of the Hydraulics Division, ASCE, 103(HY3), pp. 295-310.

[2] Blumberg, A. F., and Mellor, G. L. (1987), "A description of a three-dimensional coastal ocean circulation model in Three-Dimensional Coastal Model", Vol.4, edited by N. Heaps, American Geophysical Union, Washington, D.C.

[3] Elder, J. W. (1959), "The dispersion of marked fluid in turbulent shear flow", Jour. fo Fluid Mechanics, 5, pp. 544-560.

[4] Kim, T. I. (2002), "Estuary circulation and sedimentation process at the mouth of Gum river", Dissertation of SeungGuyn University, pp. 114-135.

[5] KORDI (1993), Ocean Environment Management Technology - Development of technology for prediction of advection and diffusion of contaminated materials, p. 81.

[6] Madala, R. V. and Piacsek, S. A. (1977), "A semi-implicit numerical model for baroclinic oceans", J. Comput. Phys., 23, pp. 167-178.

[7] MOMAF (1983), Report of short period wave measurement at Busan.

[8] MOMAF (1997), Environmental evaluation report of Busan New port development plan, pp. 139-172.

[9] Research Institute of Korea Environmental Policy & Evaluation (2003), A study on Improvement of Ocean circulation and diffusion of suspended solids prediction scheme, p. 198.

[10] Simans, T. J. (1974), "Verification of numerical models of Lake Ontario, Part I. Circulation in spring and early summer", J. Phy. Oceanogr., 4, pp. 507-523.

[11] Wang, D. and Kravitz, D. W. (1980), "A semi-implicit two-dimensional model of estuarine circulation. Journal of Physical Oceanography", 10(3): pp. 441-454.

Received 24 Navember 2006
Accepted 4 January 2006